# CHAPTER IV
# RESULTS AND DISCUSSION

To study the optimum condition of steaming which is one of the dealumination steps combining with Ga ion-exchange and silylation over dealuminated HZSM-5 for its catalytic performance in the conversion of *n*-pentane, a comprehensive characterization of surface area, pore volume, crystalline structure, and acidity of catalysts as well as the amount of coke formed on the catalysts. Furthermore, catalyst formulation will be performed in order to reduce mass diffusion limitation and coking resistance.

## 4.1 Catalyst Characterization

### 4.1.1 BET Analysis

The surface area and pore volume of the untreated HZSM-5, pre- and post-acid leaching (AcZP5) combining Ga loading (GaAcZP5 and GaAcZP20) and silylation (CLD/Ga/Ac/ZP5, CLD/Ga/Ac/ZP20, and CLD/Ga/Ac/ZT500) are summarized in Table 4.1. The results indicated that dealumination (AcZP5) could enhance surface area and total pore volume of untreated HZSM-5, but it did not adjust the pore opening of the zeolite. According to kinetic diameter of oxalic acid is larger than pore mouth of HZSM-5 therefore acid treatment could remove aluminum atom at the external surface and pore mouth region of HZSM-5, which leading to a slight enlargement of the pore opening (Lercher *et al.* 2006). Moreover, both of steaming and acid leaching (AcZP5) could improve the mesopore volume for about 2 times comparing with the untreated HZSM-5. This could be due to the generation of secondary pore structure during the removal of aluminum from the framework (Beyer *et al.* 1994). The silylation could substantial narrow or even block the pore opening of the zeolite, the surface area and pore volume of the silylated HZSM-5 (CLD/Ga/Ac/ZP5, CLD/Ga/Ac/ZP20, and CLD/Ga/Ac/ZT500) was lower than the untreated catalyst (Bauer *et al.* 2004).

**Table 4.1** BET surface area, pore volume, micropore and mesopore volume of gamma-$Al_2O_3$, the modified and extruded HZSM-5 catalysts

| Catalysts | Surface area ($m^2/g$) | Pore Volume (mL/g) | Micropore Volume (mL/g) | Mesopore Volume (mL/g) |
|---|---|---|---|---|
| HZSM-5[1] | 345 | 0.184 | 0.159 | 0.025 |
| Ac/ZP5[1] | 350 | 0.204 | 0.154 | 0.050 |
| Ga/Ac/ZP5[1] | 319 | 0.187 | 0.141 | 0.046 |
| Ga/Ac/ZP20[1] | 297 | 0.178 | 0.129 | 0.049 |
| CLD/Ga/Ac/ZP5[1] | 291 | 0.149 | 0.138 | 0.011 |
| CLD/Ga/Ac/ZP20[1] | 273 | 0.142 | 0.128 | 0.014 |
| CLD/Ga/Ac/ZT500[1] | 302 | 0.178 | 0.133 | 0.045 |
| Extruded CLD/Ga/Ac/ZP5[2] | 284 | 0.208 | 0.120 | 0.078 |
| Extruded CLD/Ga/Ac/ZP20[2] | 262 | 0.199 | 0.112 | 0.070 |
| gamma-$Al_2O_3$[2] | 291 | 0.263 | - | 0.253 |

[1]NLDFT method, [2]BJH method

Generally, NLDFT method is used for microporous material and so modified HZSM-5 catalysts were properly analyzed by this method. Figure 4.1 shows extruded CLD/Ga/Ac/ZP5 and gamma-$Al_2O_3$ considered as mesoporous material because mesopore volume was significantly high in range 20 to 500 Å of pore width. Hence, they were suitable to use BJH method to analyzing its volume because BJH method is suitable for mesoporous material.

I28368873

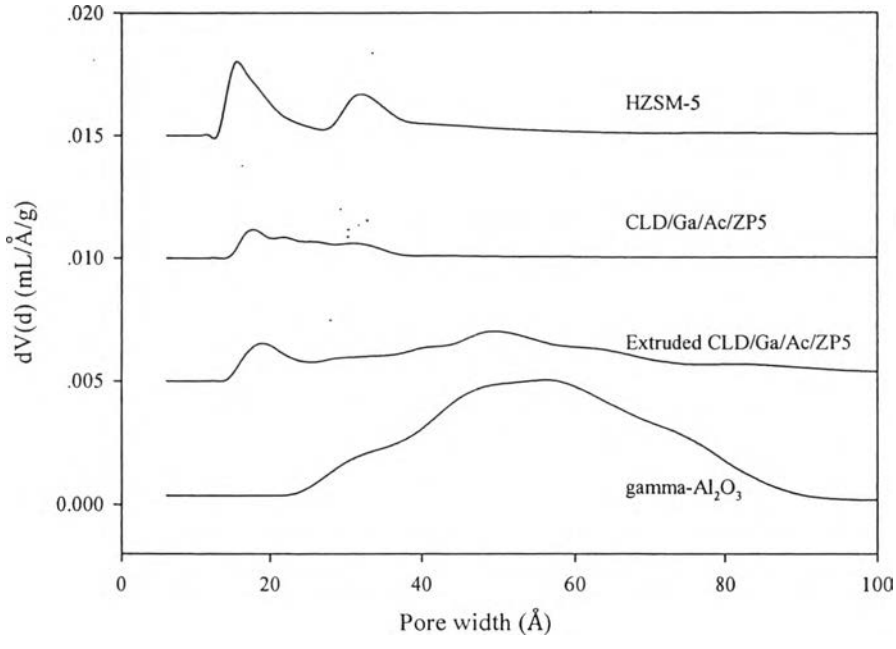


**Figure 4.1** Pore size distributions of HZSM-5, gamma- $Al_2O_3$, powdery and extruded CLD/Ga/Ac/ZP5 catalysts.

Both extruded CLD/Ga/Ac/ZP5 and CLD/Ga/Ac/ZP20 catalysts had lower surface area than their powder forms due to the water removal of AlOOH after calcination as mentioned in TGA. The pore volume of extruded CLD/Ga/Ac/ZP5 and CLD/Ga/Ac/ZP20 catalysts increased, it could be that porous gamma-$Al_2O_3$ matrices were introduced during calcination (Freiding *et al.* 2011). Gardere and co-worker in 2012 also found that the inter-particular porosity was formed due to the presence of acetic acid protons on the surface of the pseudoboehmite during peptization. This effect led to an electrostatic repulsion due to the positively charged surface.

4.1.2 X-ray Diffraction

For the effect of each treatment step, different temperatures and vapor pressures of steaming were modified over HZSM-5 catalysts. The X-ray diffraction patterns were investigated and shown in Figures 4.2 and 4.3, respectively.

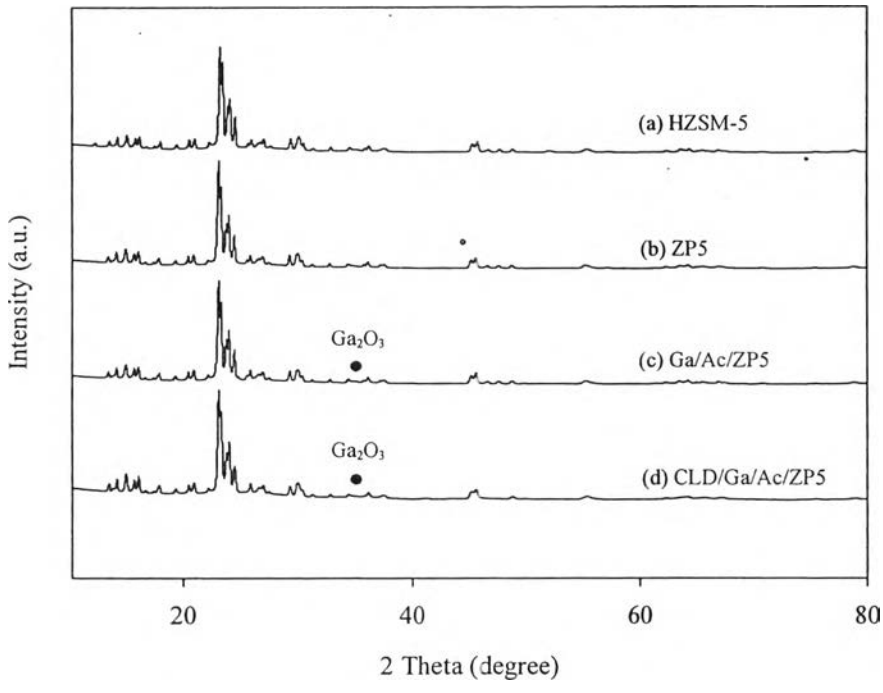


**Figure 4.2** XRD patterns of modified HZSM-5 catalysts at different treatment steps (a) HZSM-5, (b) ZP5, (c) Ga/Ac/ZP5, and (d) CLD/Ga/Ac/ZP5.

The scanning region of the diffraction angle 2θ was 10-80° which covered most of the significant diffraction peaks of the zeolite (Zhao *et al.* 2010). The XRD peaks represented the crystalline MFI structure of HZSM-5. Figure 4.2 shows that the crystal structure of the modified catalysts was unchanged with the steaming, acid leaching, Ga ion-exchange, and silylation. The high intensity of peaks in the XRD patterns indicated highly crystalline of the zeolite samples. The intensities of the peaks at 2θ = 24° of pre-acid leaching and steaming (ZP5) increased slightly because of the removal of framework aluminum (Ding *et al.* 2007). No new diffraction peaks were observed in the Ga ion-exchanged catalysts (Ga/Ac/ZP5). This could be indicated that gallium was highly dispersed on the HZSM-5 catalysts. Furthermore, the structure and the relative crystallinity of the catalysts were unchanged after silylation treatment (CLD/Ga/Ac/ZP5).

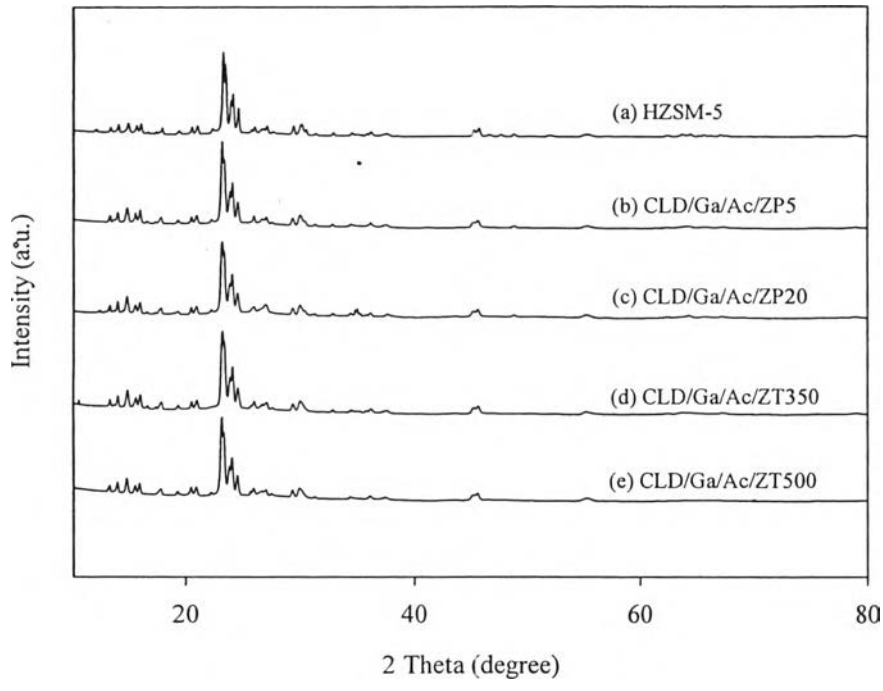


**Figure 4.3** XRD patterns of silylation after Ga loading, pre- and post-acid leaching of steaming over modified HZSM-5 catalysts (a) HZSM-5, (b) CLD/Ga/Ac/ZP5, (c) CLD/Ga/Ac/ZP20, (d) CLD/Ga/Ac/ZT350, and (e) CLD/Ga/Ac/ZT500.

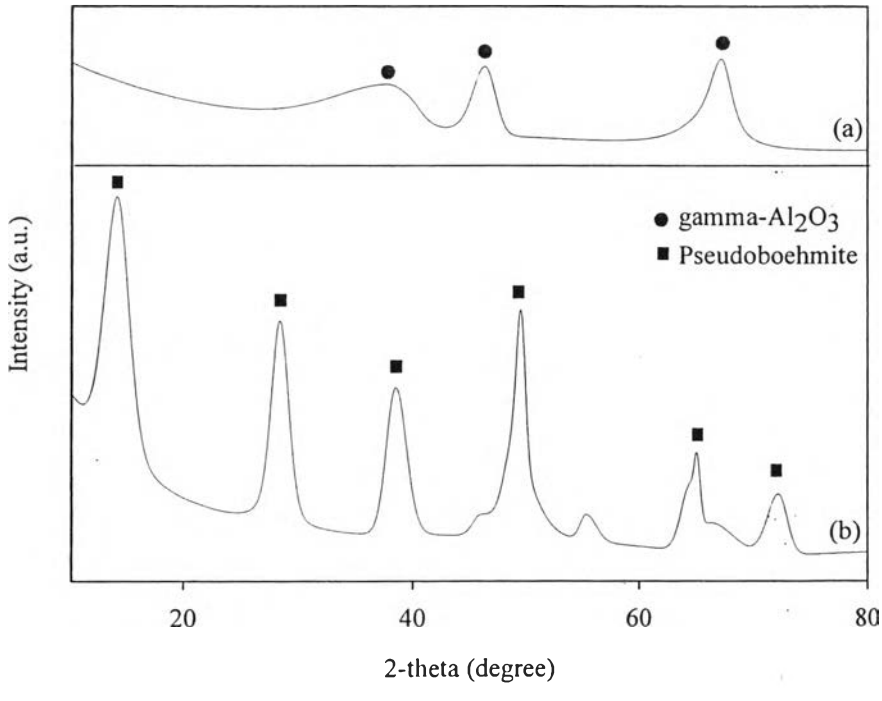


(a) Calcined pseudoboehmite at 500 $^{o}$C
(b) Uncalcined pseudoboehmite at room temperature

**Figure 4.4** XRD patterns of pseudoboehmite at room temperature and 500 °C.

The gamma-AlOOH was transformed to gamma-$Al_2O_3$ after calcination as shown in Figure 4.4. After extrusion, the crystallinity of HZSM-5 did not change but intensity slightly decreased as shown in Figure 4.5. The extruded CLD/Ga/Ac/ZP5 and CLD/Ga/Ac/ZP20 catalysts did not show the peak at 2-theta of 67 degree being one of gamma-$Al_2O_3$ peaks (Garderen *et al.* 2012). The XRD intensity of gamma- $Al_2O_3$ was very small and broad compared with HZSM-5 so that XRD patterns of extruded catalysts were hidden by those of HZSM-5 catalyst (Kim *et al.* 2006).

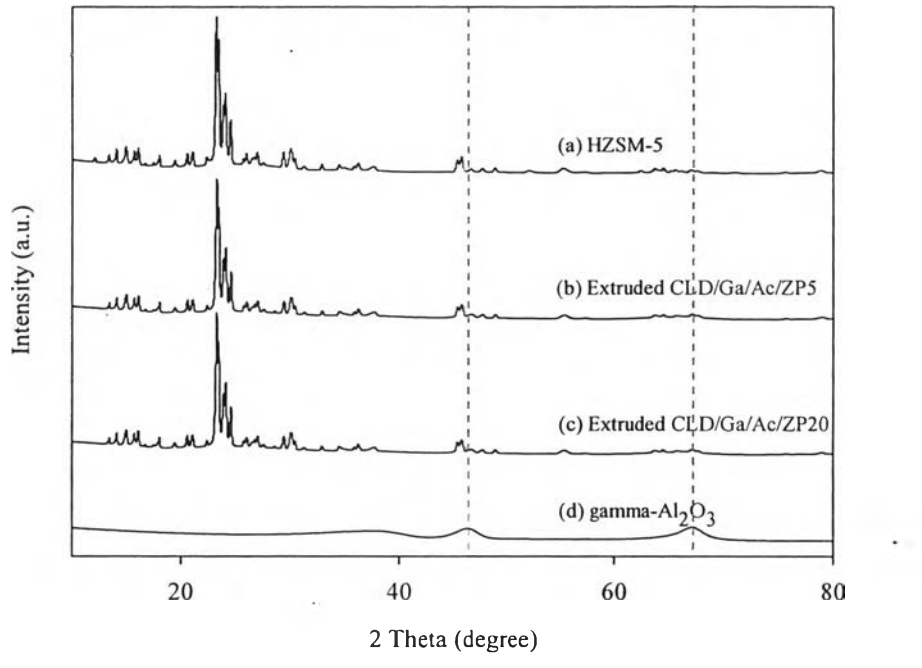


**Figure 4.5** XRD patterns of extruded HZSM-5 catalysts and gamma-$Al_2O_3$. (a) HZSM-5, (b) extruded CLD/Ga/Ac/ZP5, (c) extruded CLD/Ga/Ac/ZP20, and (d) gamma-$Al_2O_3$.

4.1.2 TPD of Isopropylamine

The Brønsted acid sites of untreated HZSM-5 and modified HZSM-5 (dealumination, Ga ion-exchange, and silylation) are summarized in Table 4.2. The results indicated that the acid sites of dealuminated HZSM-5 (Ac/ZP5 and Ac/ZP20) increased compared with the untreated HZSM-5. It could be due to the realumination process (Lin *et al.* 2007). After reducing Ga/Ac/ZP5 and Ga/Ac/ZP20 catalysts with $H_2$, acidities were lower than unloaded Ga catalysts due to replacement of

exchangeable cations $Ga^{+}$ in HZSM-5 framework. The reduction of octahedrally coordinated $Ga^{3+}$ ions was formed to reduced univalent $Ga^{+}$ ions (Ausavasukhi *et al.* 2009). For all of reduced silylation HZSM-5 catalysts, Brønsted acidities greatly decreased due to the coverage of deposition silica on the external surface of zeolite. In agreement with Zhu and co-worker in 2007, the deactivation of the active sites and blockage of pore opening on external surface were found from silylation treatment over HZSM-5.

**Table 4.2** Brønsted acidity of the modified HZSM-5 catalysts prepared by steaming, acid leaching, Ga ion-exchange, and silylation from TPD-IPA

| Catalysts | Brønsted acidity (μmol/g) |
|---|---|
| HZSM-5 | 658 |
| Ac/ZP5 | 764 |
| Ga/Ac/ZP5 | 301 |
| CLD/Ga/Ac/ZP5 | 290 |
| Ac/ZP20 | 678 |
| Ga/Ac/ZP20 | 380 |
| CLD/Ga/Ac/ZP20 | 234 |
| CLD/Ga/Ac/ZP40 | 266 |
| CLD/Ga/Ac/ZT350 | 272 |
| CLD/Ga/Ac/ZT500 | 323 |
| CLD/Ga/Ac/ZT650 | 259 |
| Extruded CLD/Ga/Ac/ZP5 | 277 |
| Extruded CLD/Ga/Ac/ZP20 | 223 |
| gamma-$Al_2O_3$ | 68 |

From Figure 4.6, the mild steaming treatment (Ac/ZP5 and Ac/ZP20) enhanced the strength of Brønsted acid sites of HZSM-5 because proton required lower temperature to start Hofmann elimination reaction. Niwa and co-worker in

2012 found that mild steaming increased the strength of Brønsted acid sites with increasing partial pressure of water vapor less than 20 kPa under atmospheric pressure. From Figure 4.7, only CLD/Ga/Ac/ZP5 and CLD/Ga/Ac/ZP20 catalysts were still strong strength of Brønsted acid sites which was facilitated high *n*-pentane conversion and aromatic selectivity.

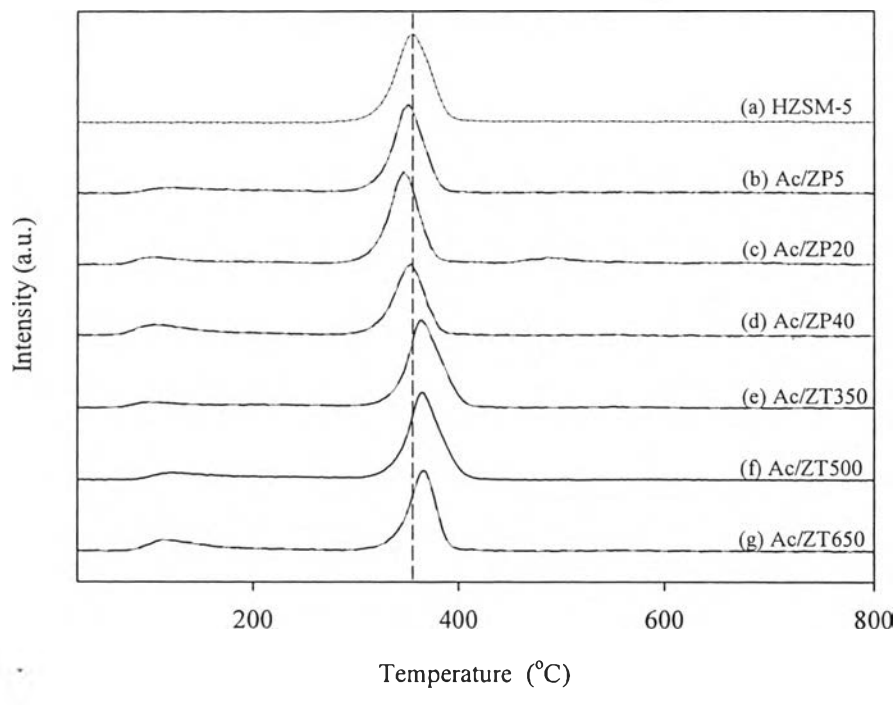


**Figure 4.6** TPD profiles of pre- and post- acid leaching of steaming over modified HZSM-5 catalysts (a) HZSM-5, (b) Ac/ZP5, (c) Ac/ZP20, (d) Ac/ZP40, (e) Ac/ZT350, (f) Ac/ZT500, and (g) Ac/ZT650.

Table 4.2 shows that the number of Brønsted acidities was lower in extrudates due to lower zeolite contents. Lee and co-worker in 2010 also found that gamma-$Al_2O_3$ binder diluted strong acid sites of HZSM-5 catalysts. Therefore, both extruded CLD/Ga/Ac/ZP5 and CLD/Ga/Ac/ZP20 catalysts were weaker Brønsted acidic strength compared to their powdery forms because of the peak shifted to a higher temperature (Kim *et al.* 2006) as shown in Figure 4.8.

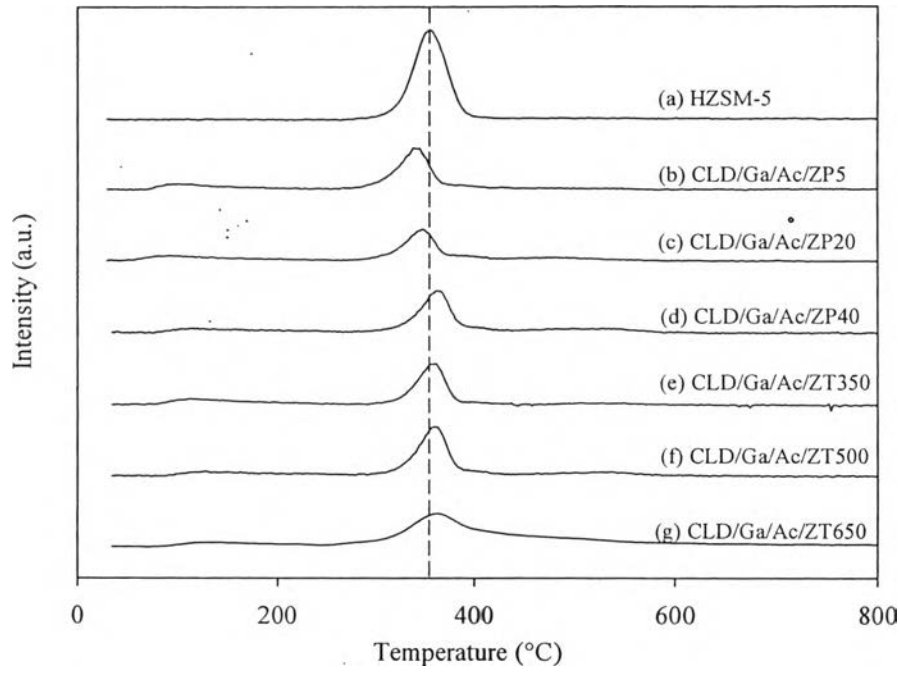


**Figure 4.7** TPD profiles of unmodified and modified HZSM-5 catalysts (a) HZSM-5, (b) CLD/Ga/Ac/ZP5, (c) CLD/Ga/Ac/ZP20, (d) CLD/Ga/Ac/ZP40, (e) CLD/Ga/Ac/ZT350, (f) CLD/Ga/Ac/ZT500, and (g) CLD/Ga/Ac/ZT650.

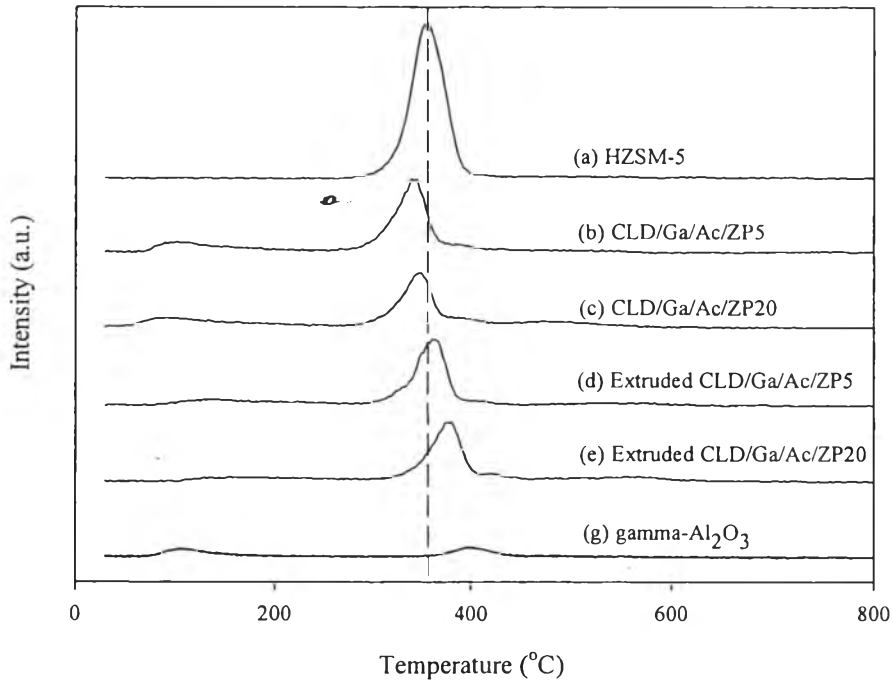


**Figure 4.8** TPD profiles of gamma-$Al_2O_3$, modified and extruded HZSM-5 catalysts (a) HZSM-5, (b) extruded CLD/Ga/Ac/ZP5, (c) extruded CLD/Ga/Ac/ZP20, and (d) gamma-$Al_2O_3$.

4.1.4 TPR

Temperature programmed ($H_2$) reduction (TPR) profiles of silylation and Ga loading over dealuminated HZSM-5 are shown in Figure 4.9. The Ga/Ac/ZP5 and Ga/Ac/ZP20 catalysts showed peak at 650 °C due to reduction of $Ga_2O_3$ to $Ga_2O$. Later, $Ga_2O$ became exchangeable cations with negative charge of zeolite leading to lower Brønsted acidities in Table 4.2.

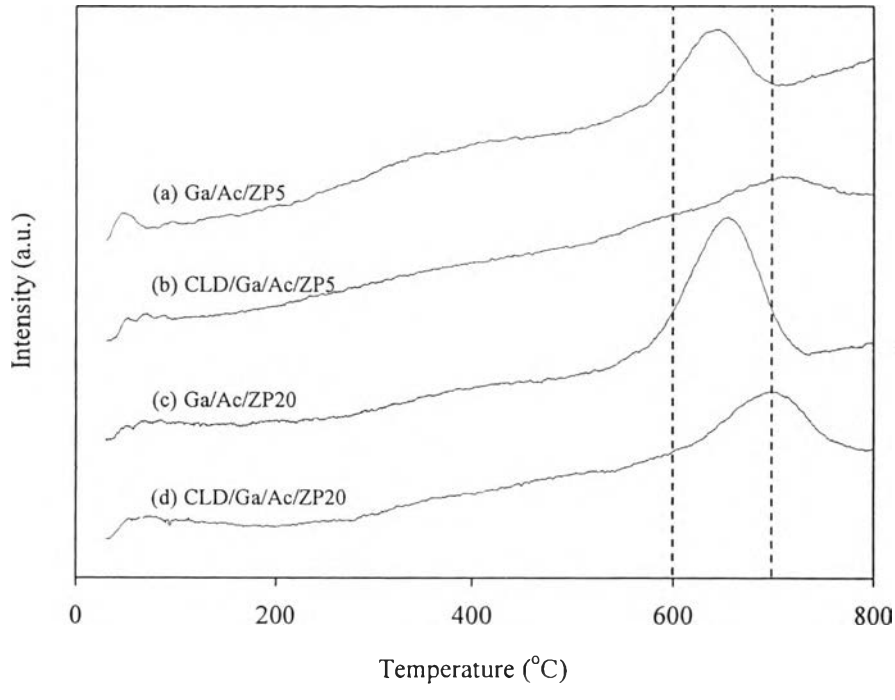


**Figure 4.9** TPR profiles of modified HZSM-5 catalysts (a) Ga/Ac/ZP5, (b) CLD/Ga/Ac/ZP5, (c) Ga/Ac/ZP20, and (d) CLD/Ga/Ac/ZP20.

After silylation, both of CLD/Ga/Ac/ZP5 and CLD/Ga/Ac/ZP20 catalysts performed peak at 700 °C because the large $Ga_2O_3$ weakly interacted with zeolite matrixes (Ausavasukhi *et al.* 2009). The deposited silicon compound could block some external surfaces and pore mouth opening of silylated HZSM-5 catalysts. The low surface area and amount of Brønsted acid sites are confirmed in Tables 4.1 and 4.2, respectively.

4.1.5 Scanning Electron Microscopy (SEM)

Scanning electron microscopy was used to investigate the surface modification of untreated HZSM-5, silylation, Ga ion-exchange, and extruded CLD/Ga/Ac/ZP5 catalysts in Figure 4.10. The morphology of HZSM-5 and Ga/Ac/ZP5 catalysts was similar. It could be Ga well-dispersed on HZSM-5 external surface in agreement with no $Ga_2O_3$ peak from XRD result in Figure 4.2. The silylated HZSM-5 (CLD/Ga/Ac/ZP5) had dense layer of amorphous silica on the external surface (Hui *et al.* 2011). It was suggested that a layer deposition was a dense of amorphous silica due to the silylation treatment. Thus, deposition of an inert silica layer deactivated external acid sites resulting high *p*-xylene selectivity in xylenes as shown in Table 4.9. After extrusion, extruded CLD/Ga/Ac/ZP5 catalyst was covered with some gamma-$Al_2O_3$ particles on external surface.

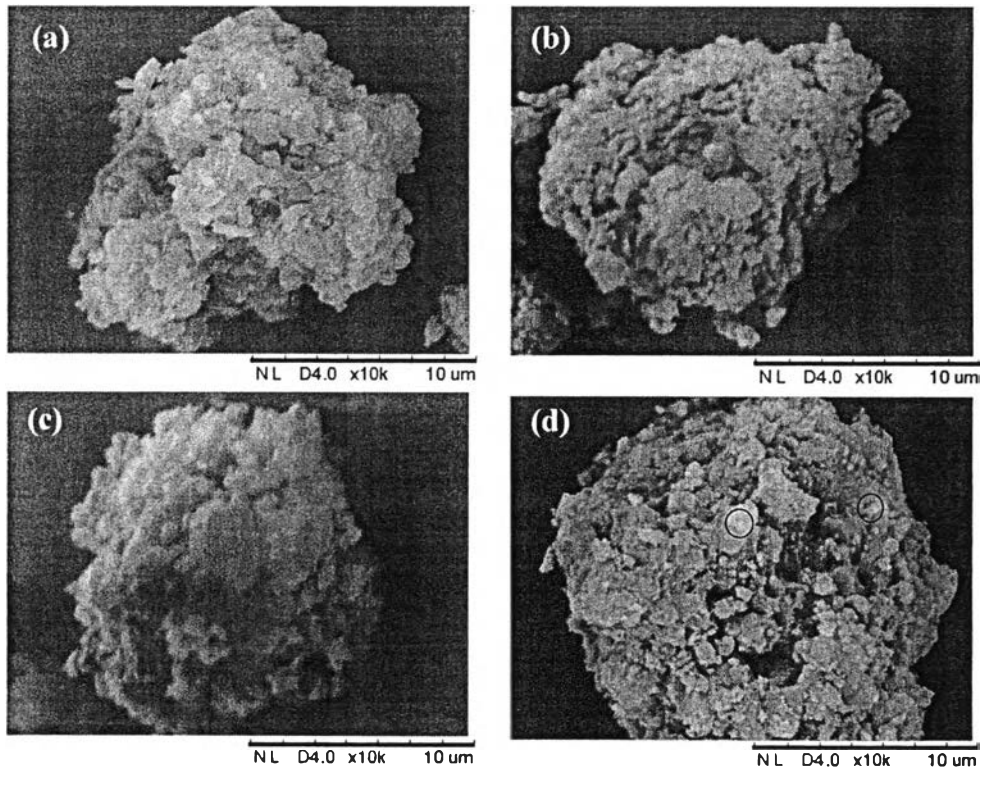


**Figure 4.10** SEM images of modified and extruded HZSM-5 catalysts (a) HZSM-5 (b) Ga/Ac/ZP5, (c) CLD/Ga/Ac/ZP5, and (d) Extruded CLD/Ga/Ac/ZP5.

4.1.6 Themogravimetry Analysis

The themogravimetry analysis method was used to investigate the mass loss behavior at the elevated temperature of samples.

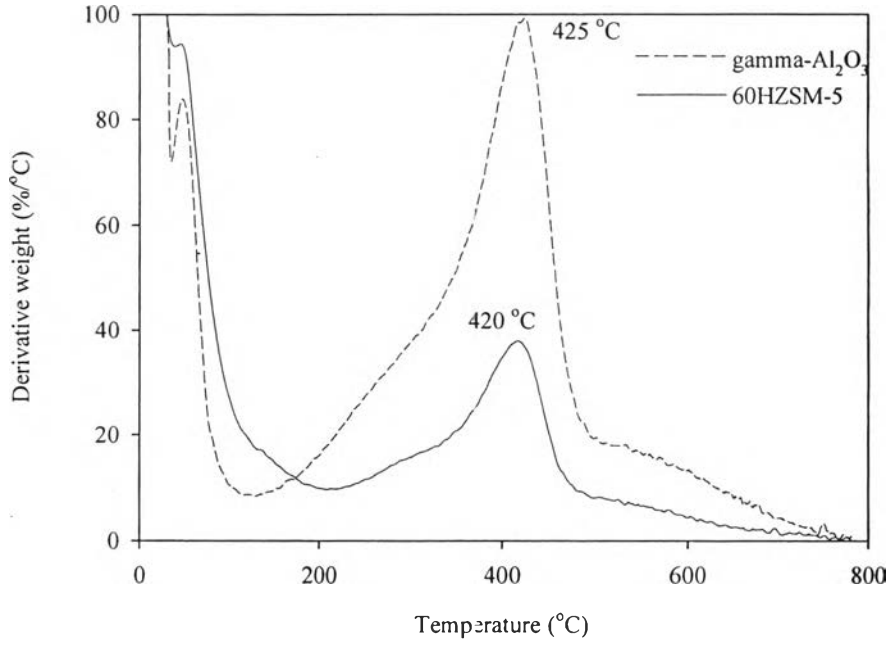


**Figure 4.11** Derivative thermogravimetry analysis (DTG) curve of extruded 60HZSM-5 catalyst and gamma-$Al_2O_3$.

According to Figure 4.11, the extruded pseudoboehmite binder and 60HZSM-5 catalyst had weight loss two stages. In the first stage, the desorption of physisorbed water and residual acetic acid were observed from the pseudoboehmite particle surface. The second stage corresponded to the desorption of chemisorbed water to the Al groups, the decomposition of the organic groups, and OH diffusion from the surface of the material. It could be dehydration of OH groups during the phase transition from gamma-AlOOH to gamma-$Al_2O_3$ (Kaya *et al.* 2002). The weight loss in the second stage might be the presence of $Al(OH)(OAc)_2$ or $Al_2O_{2.9}(OAc)_{0.17}{\cdot}1.9H_2O$ with Ac as the acetyl group (Tregubenko *et al.* 2011). The extruded pseudoboehmite binder exhibited higher weight loss than extruded 60HZSM-5 catalyst due to phase transition from gamma-AlOOH to gamma-$Al_2O_3$

(Fauchadour *et al.* 2000). In addition, the transformation from pseudoboehmite to gamma-$Al_2O_3$ was confirmed by XRD in Figure 4.4.

4.1.7 Mechanical Testing

The acetic acid concentration and calcination temperature affected the strength of extruded HZSM-5 catalyst because porosity was formed after drying.

**Table 4.3** Radial crushing strength of pseudoboehmite with varied acetic acid concentration at 500 °C calcination temperature

| Acetic acid concentration (vol %) | Radial crushing strength (N/cm) |
|---|---|
| 1% | 119.4 |
| 2% | 141.0 |
| 3% | 151.0 |
| 4% | 112.6 |
| 5% | 84.3 |

The acetic concentration was varied from 1 to 5 vol% at 500 °C calcination temperature (Saxena *et al.* 2013). Table 4.3 shows that 3 vol% acetic acid concentration exhibited the highest radial crushing strength at 151.0 N/cm. Lamberov and co-worker in 2003, they found that formation of partial dissolution of basic aluminium salt enhanced the mechanical strength of the grains. For attrition resistance, low acid concentration was benefits because of the closer contact between particles after decomposition. In agreement with Garderen and co-worker in 2012, low acid concentration was not formed salt which enhanced the fragility in the material resulting in a decrease in contact point after decomposition between pseudoboehmite particles (Garderen *et al.* 2012).

The calcined temperature was studied under 650 °C which was the maximum calcined temperature maintaining HZSM-5 zeolite structure. The calcined temperature was varied from 500 to 650 °C with extruded pseudoboehmite preparing 3 vol% acetic acid concentration. Table 4.4 shows that the extrudates performed the highest radial crushing strength at 158.6 N/cm at 550 °C calcination temperature.

**Table 4.4** Radial crushing strength of pseudoboehmite preparing 3 vol% acetic acid concentration with varied calcination temperature

| Calcined temperature (°C) | Radial crushing strength (N/cm) |
|---|---|
| 500 | 151.0 |
| 550 | 158.6 |
| 600 | 131.3 |
| 650 | 106.8 |

Hence, the extruded HZSM-5 catalysts were prepared with 3 vol% acetic acid concentration and 550 °C calcination temperature.

**Table 4.5** Physical and mechanical properties of extruded HZSM-5 catalysts

| Component | Unit | Extrudates | | | | |
|---|---|---|---|---|---|---|
| | | Pseudo-boehmite | 60 HZSM-5 | 80 HZSM-5 | CLD/Ga/ Ac/ZP5 | CLD/Ga/ Ac/ZP20 |
| HZSM-5 | wt% | 0.0 | 65.7 | 86.5 | 87.6 | 87.0 |
| Pseudoboehmite | wt% | 100.0 | 34.3 | 13.5 | 12.4 | 13.0 |
| Diameter | mm | 1.8 | 1.8 | 1.8 | 1.8 | 1.8 |
| Length | mm | 4.2 | 4.0 | 4.0 | 4.0 | 4.2 |
| Bulk density | $g/cm^3$ | - | - | 0.60 | - | - |
| Attrition loss | wt% | - | - | 0.73 | - | - |
| Radial crushing strength | N/cm | 158.6 | 106.2 | 75.2 | 65.7 | 62.4 |

All extruded HZSM-5 with pseudoboehmite binder showed lower strength than pseudoboehmite because the peptization leaded the absence of coagulation contact between zeolite and binder.

**Table 4.6** Physical and mechanical properties of commercially extruded catalysts

| Commercial catalysts | Diameter (mm) | Length (mm) | Radial crushing strength (N/cm) |
|---|---|---|---|
| $CuOZnO-Al_2O_3$ | 4.8 | 3.0 | 299.4 |
| $CoMo-Al_2O_3$ | 1.2 | 5.1 | 168.0 |

## 4.2 Catalytic Activity Testing

The untreated and modified HZSM-5 catalysts were tested for their catalytic activity and aromatic selectivity in converting *n*-pentane. The obtained products could be classified into three main groups; (1) light paraffins: methane, ethane, propane, and butane, (2) light olefins: ethylene, propylene, acetylene, 1-butene, and iso-butene, and (3) aromatics: benzene, toluene, ethylbenzene, *p*-xylene, *m*-xylene, and *o*-xylene.

### 4.2.1 Effect of Pre- and Post-acid Leaching of Steaming over HZSM-5

The untreated HZSM-5 zeolite preparing with pre-acid leaching (Ac/HZSM-5), followed by steaming (ZT500), and post-acid leaching (Ac/ZT500) were tested in aromatization of *n*-pentane for their catalytic performances. Product selectivity and conversion of *n*-pentane are compared in Figure 4.12. From Table 4.7, HZSM-5 provided conversion around 87%, while Ac/ZT500 had a conversion of 92%. This improvement could be due to the generated mesopore and totally removed extra framework Al out of zeolite structure. In case of Ac/HZSM-5, it showed lower conversion at 80% because extra framework Al species still plugged in zeolite structure which was not active sites for aromatization. However, acid leaching removed extra framework aluminums (EFAL) out of zeolite structure (Muller *et al.* 2000). Furthermore, the aromatics selectivity showed the same trend as conversion but not influenced to *p*-xylene selectivity in xylenes. All of catalysts in Figure 4.12, the *p*-xylene selectivity in xylenes was about 24% which was close to its thermodynamic equilibrium (24% *o*-xylene, 53% *m*-xylene, and 23% *p*-xylene). *p*-Xylene was isomerized to *m*-xylene and *o*-xylene before escaping the pores of HZSM-5. In agreement with Hui and co-worker in 2011, they concluded that the dealumination by acid treatment did not affect the *p*-xylene selectivity.

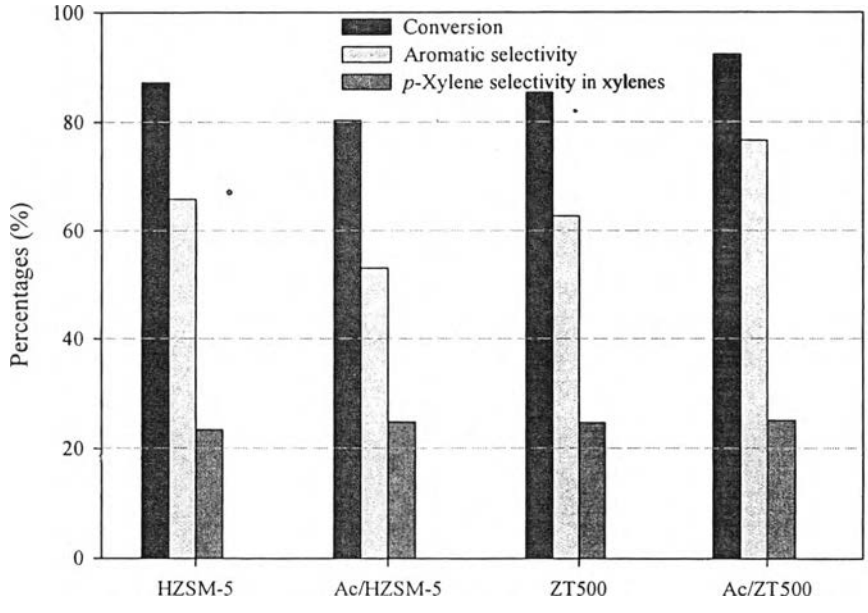


**Figure 4.12** Effect of pre- and post-acid leaching of steaming (temperature 500 °C and partial pressure of steaming of 26.75 kPa) over HZSM-5 catalysts for the *n*-pentane conversion, aromatic selectivity, and *p*-xylene selectivity in xylenes. (Reaction condition: 500 °C, 1 atm, WHSV = 5 $h^{-1}$, and TOS = 440 min)

**Table 4.7** Product selectivity and conversion of *n*-pentane over unmodified HZSM-5, Ac/HZSM-5, ZT500, and Ac/ZT500 catalysts (Reaction condition: 500 °C, 1 atm, WHSV = 5 $h^{-1}$, and TOS = 440 min)

| Products | Catalysts | | | |
|---|---|---|---|---|
| | HZSM-5 | Ac/HZSM-5 | ZT500 | Ac/ZT500 |
| Light paraffins | 16.07 | 25.08 | 15.96 | 11.78 |
| Light olefins | 9.43 | 11.15 | 13.36 | 7.55 |
| Benzene | 5.78 | 3.71 | 5.92 | 6.98 |
| Toluene | 28.48 | 20.97 | 30.18 | 38.40 |
| Ethylbenzene | 1.77 | 2.24 | 1.42 | 2.20 |
| Xylenes | 23.94 | 19.37 | 16.03 | 23.32 |
| Aromatics selectivity | 68.69 | 53.14 | 62.71 | 75.05 |
| Conversion | 87.29 | 80.36 | 85.42 | 92.45 |
| *p*-Xylene selectivity in xylenes | 23.44 | 24.83 | 24.74 | 25.45 |
| *p*-Xylene yield | 4.90 | 3.86 | 3.39 | 4.90 |

**Table 4.8** The amount of coke on the HZSM-5, Ac/HZSM-5, ZT500, and Ac/ZT500 catalysts after 440 min time on stream (Reaction condition: 500 °C, 1 atm, and WHSV = 5 $h^{-1}$)

| Catalysts | Coke (wt%) |
|---|---|
| HZSM-5 | 7.7 |
| Ac/HZSM-5 | 4.9 |
| ZT500 | 3.6 |
| Ac/ZT500 | 3.4 |

Temperature programmed oxidation technique was used to analyze the amount of the coke deposition on the spent catalysts. As shown in Table 4.8, the higher amount of coke was observed on the HZSM-5 of 7.7 wt% comparing with Ac/ZT500 of 3.4 wt%. The nature of coke was analyzed by TPO as shown in Figure 4.13. The coke profiles of spent catalysts had three ranges. Firstly, it might be some bulky hydrocarbons at external surface below 200 °C. Another, low temperature (200-450 °C) and high temperature (450-600 °C) was soft coke and hard coke, respectively.

4.2.2 Effect of Steaming over Modified HZSM-5

The silylation treatment by chemical liquid deposition (CLD) with TEOS could enhance *p*-xylene selectivity due to the deactivation at external acid sites of zeolite (Hui *et al.* 2011). However, external surface acid sites and pore-narrowing of the zeolite suppressed catalytic activity simultaneously (Bauer *et al.* 2004). Figure 4.14 shows the *n*-pentane conversion, aromatic selectivity, and *p*-xylene selectivity in xylenes. Products distribution showed 63 %*p*-xylene selectivity in xylenes for both of CLD/Ga/Ac/ZP5 and CLD/Ga/Ac/ZP20 catalysts in Table 4.9, Moreover, both of modified catalysts performed good stability in Figure 4.15 and low coke deposition as shown in Table 4.10.

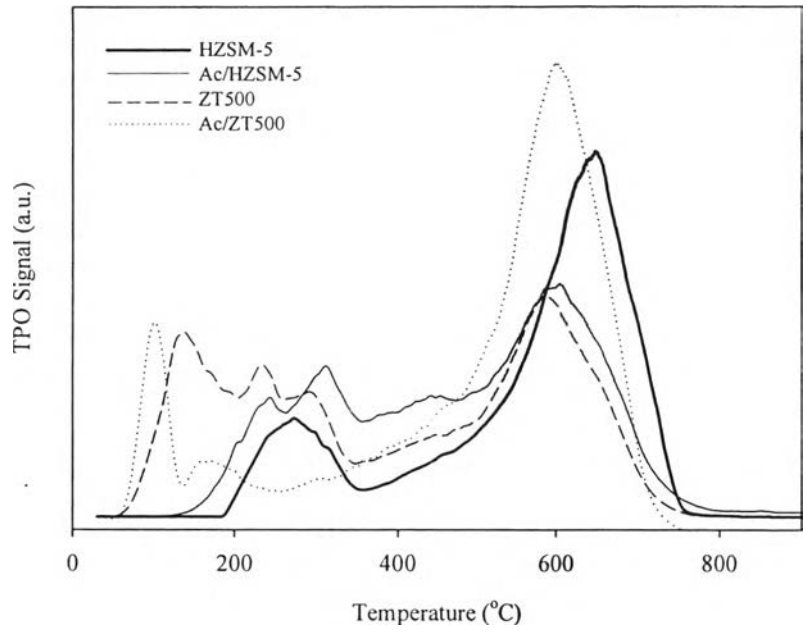


**Figure 4.13** Temperature programmed oxidation (TPO) profiles of spent catalysts after 440 min time on stream. (Reaction condition: 500 °C, 1 atm, and WHSV = 5 $h^{-1}$)

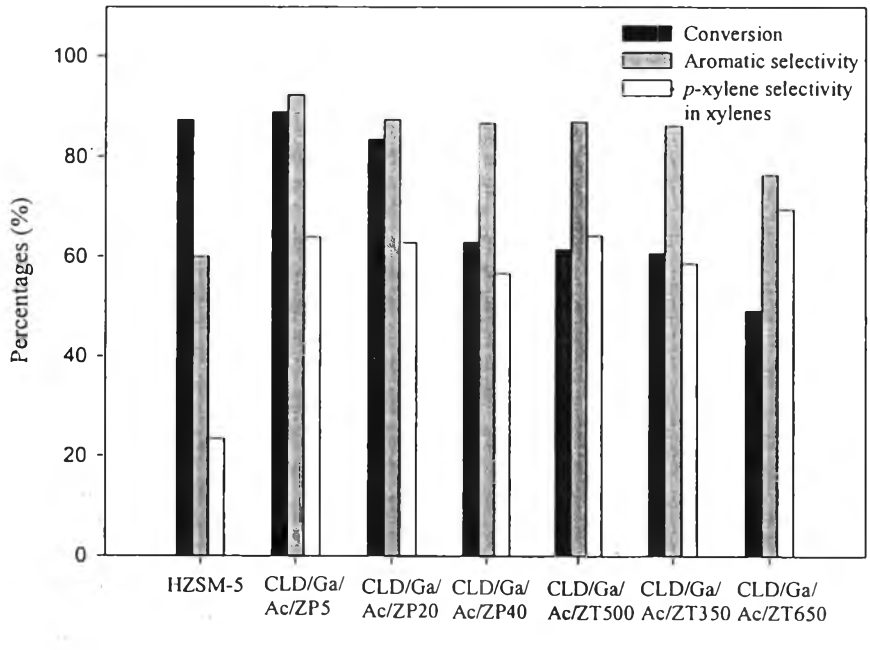


**Figure 4.14** Effect of steaming condition over modified HZSM-5 catalysts on the *n*-pentane conversion, aromatic selectivity, and *p*-xylene selectivity in xylenes. (Reaction condition: 500 °C, 1 atm, WHSV = 5 $h^{-1}$, and TOS = 440 min)

**Table 4.9** Product selectivity and conversion of *n*-pentane over modified HZSM-5 catalysts by silylation, Ga ion-exchange, and dealumination (Reaction condition: 500 °C, 1 atm, WHSV = 5 $h^{-1}$, and TOS = 440 min)

| Products | Catalysts | | | | | | |
|---|---|---|---|---|---|---|---|
| | HZSM-5 | CLD/ Ga/ Ac/ ZP5 | CLD/ Ga/ Ac/ ZP20 | CLD/ Ga/ Ac/ ZT350 | CLD/ Ga/ Ac/ ZT500 | CLD/ Ga/ Ac/ ZP40 | CLD/ Ga/ Ac/ ZT650 |
| Light paraffins | 16.07 | 0.35 | 1.52 | 1.60 | 0.84 | 1.37 | 0.82 |
| Light olefins | 9.43 | 5.09 | 7.45 | 5.31 | 5.24 | 4.89 | 8.23 |
| Benzene | 5.78 | 14.74 | 12.18 | 6.98 | 5.31 | 5.44 | 6.15 |
| Toluene | 28.48 | 40.09 | 36.13 | 31.52 | 24.70 | 26.70 | 19.45 |
| Ethylbenzene | 1.77 | 3.01 | 2.46 | 2.27 | 2.91 | 2.87 | 1.56 |
| Total Xylenes | 23.94 | 24.23 | 22.08 | 20.75 | 20.51 | 19.52 | 10.39 |
| *p*-Xylene | 5.61 | 15.50 | 13.88 | 12.65 | 13.17 | 11.06 | 7.22 |
| *m*-Xylene | 13.22 | 7.41 | 6.88 | 6.83 | 6.32 | 7.04 | 2.80 |
| *o*-Xylene | 5.10 | 1.32 | 1.32 | 1.26 | 1.01 | 1.43 | 0.36 |
| Others | 14.53 | 12.49 | 18.18 | 31.58 | 40.51 | 39.22 | 53.40 |
| Aromatics selectivity | 68.69 | 92.27 | 87.32 | 86.15 | 86.90 | 86.62 | 76.41 |
| Aromatics yield | 59.96 | 82.07 | 72.85 | 61.52 | 54.52 | 54.52 | 37.54 |
| Conversion | 87.29 | 88.94 | 83.43 | 71.40 | 62.94 | 62.94 | 49.13 |
| *p*-Xylene selectivity in xylenes | 23.44 | 63.96 | 62.87 | 60.99 | 64.23 | 56.64 | 69.56 |
| *p*-Xylene yield | 4.90 | 13.78 | 11.58 | 9.04 | 8.29 | 6.96 | 3.55 |

4.2.3 Effect of Ga Ion-exchange and Silylation

It is the fact that the presence of Ga could improve dehydrogenation reaction enhancing aromatization activity. Further narrowing of the pore opening of zeolite was done by silylation via chemical liquid deposition. Gallium improved aromatic selectivity because it suppressed the strength of Brønsted acid sites (Kimura *et al.* 2012). The $Ga^{+}$ species were formed after reducing with $H_2$ because $Ga^{3+}$ mainly located at the external surface of zeolite due to larger diameter than pore opening of zeolite (El-Malki *et al.* 2000). For aromatics products, toluene was the dominant ones. Table 4.9 shows that every modified HZSM-5 catalysts distributed more aromatics products than untreated HZSM-5 catalyst. The CLD/Ga/Ac/ZP5 catalysts exhibited the highest *p*-xylene yield at 13.8% comparing with other

modified catalysts. For stability at Figure 4.15, the CLD/Ga/Ac/ZP5 catalyst performed similarly conversion with the CLD/Ga/Ac/ZP20 catalyst. In agreement with Niwa and co-worker in 2012, the mild steaming condition was suitable for *n*-pentane aromatization and coking resistance due to mesopore generation (Nagamori *et al.* 1998) as shown in Table 4.1.

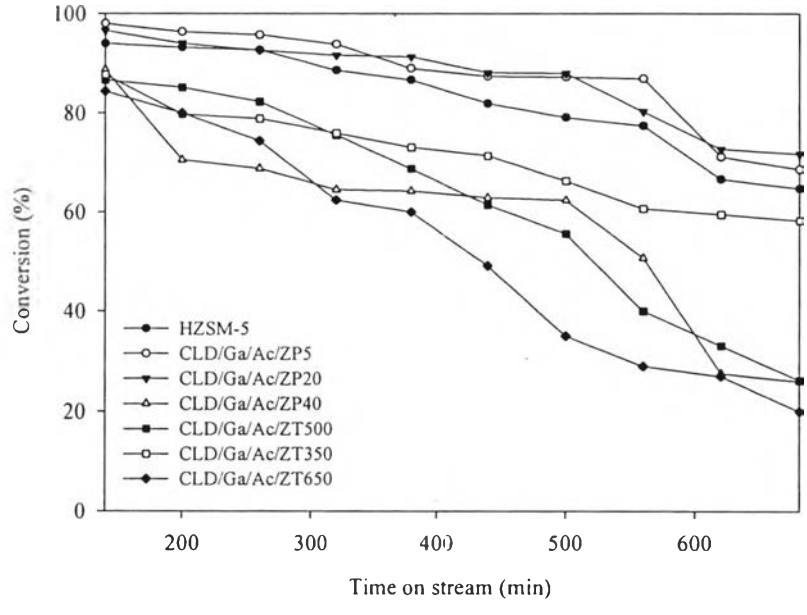


**Figure 4.15** Stability on conversion of *n*-pentane over modified (dealumination, Ga ion-exchange, and silylation) HZSM-5 catalysts. (Reaction conditions: 500 °C, 1 atm, and WHSV = 5 $h^{-1}$)

**Table 4.10** The amount of coke on the unmodified and modified HZSM-5 catalysts after 440 min time on stream (Reaction condition: 500 °C, 1 atm, and WHSV = 5 $h^{-1}$)

| Catalysts | Coke (wt%) |
|---|---|
| HZSM-5 | 7.7 |
| CLD/Ga/Ac/ZP5 | 4.3 |
| CLD/Ga/Ac/ZP20 | 6.4 |
| CLD/Ga/Ac/ZP40 | 7.2 |
| CLD/Ga/Ac/ZT350 | 3.8 |
| CLD/Ga/Ac/ZT500 | 4.0 |
| CLD/Ga/Ac/ZT650 | 2.8 |

The coke normally was formed over the catalyst and might cover some of acid sites or block the pore opening of the zeolite resulting catalyst deactivation. Table 4.10 shows that all modified HZSM-5 catalysts showed lower amount of coke than unmodified HZSM-5 catalyst (7.7 wt%). It could be that the Brønsted acidity of all modified HZSM-5 catalyst was lower compared to untreated HZSM-5 (658 μmol/g) resulting highest coke formation.

### 4.3 Catalyst Formulation Activity Testing

The purposes of shaping were properly catalytic activity and sufficient mechanical properties. The zeolite to pseudoboehmite ratios were varied at 60:40 wt% (60HZSM-5) and 80:20 wt% (80HZSM-5). For activity testing, the amount of catalyst based on zeolite content was used in order to compare activity testing before and after shaping. Therefore, amount of extrude 80HZSM-5 catalyst was lower than extrude 60HZSM-5 catalyst. Figure 4.16 shows that the extruded 80HZSM-5 catalyst had higher conversion than extruded 60HZSM-5 catalyst, it could be due to lower binder contents. Therefore, the ratio of zeolite to pseudoboehmite at 80:20 by weight was selected to be formulated as extrudates in cylindrical form.

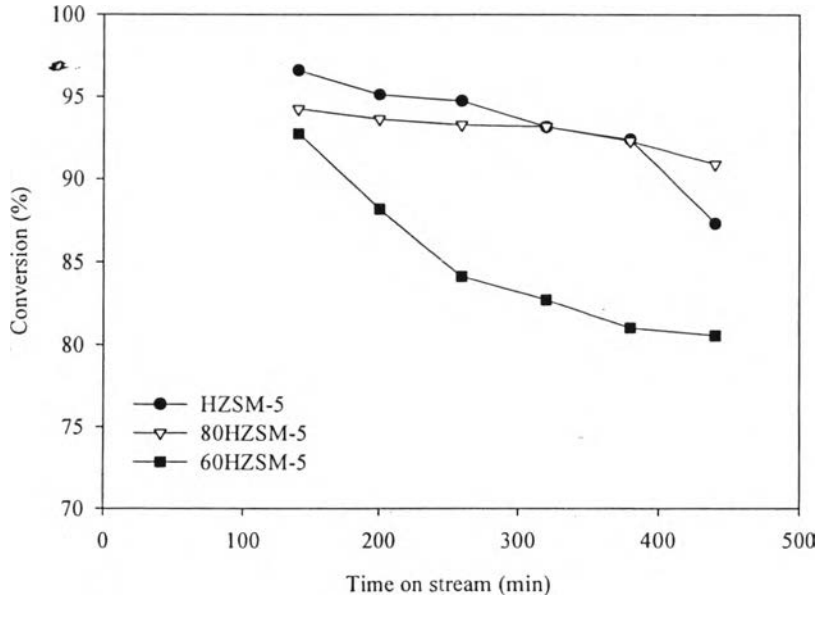


**Figure 4.16** Conversion of *n*-pentane over extruded 80HZSM-5 and 60HZSM-5 catalysts. (Reaction conditions: 500 °C, 1 atm, and WHSV = 5 $h^{-1}$)

The powdery CLD/Ga/Ac/ZP5 and CLD/Ga/Ac/ZP20 catalysts were selected to be shaped because of high conversion and aromatic selectivity as shown in Figure 4.14. After shaping, extruded CLD/Ga/Ac/ZP5 and CLD/Ga/Ac/ZP20 catalysts performed 86.5 and 78.9 %conversion, respectively. Table 4.11 shows that the extruded CLD/Ga/Ac/ZP5 catalyst had higher *p*-xylene yield (12.5 %) than the extruded CLD/Ga/Ac/ZP20 catalyst (9.4 wt%). It could be that the extruded CLD/Ga/Ac/ZP5 catalyst had higher Brønsted acidity (277 μmol/g) and stronger strength than the extruded CLD/Ga/Ac/ZP20 catalyst (223 μmol/g) as shown in Figure 4.8. After extrusion, *p*-xylene yield decreased because isomerization of *p*-xylene to be *m*- and *o*-xylene at gamma-$Al_2O_3$ binder which was proven in Table 4.12 and Figure 4.18. In agreement with Bhat and co-worker in 1995, they found that gamma-$Al_2O_3$ acidity helped *p*-xylene isomerization reaction.

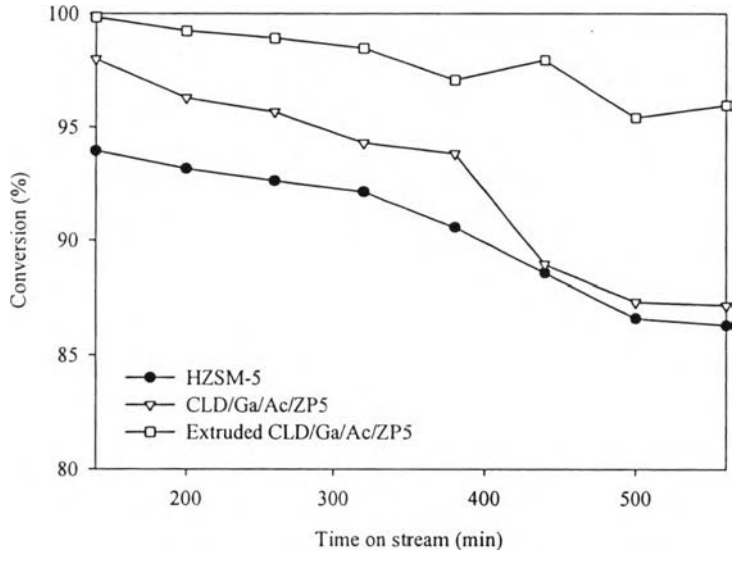


**Figure 4.17** Stability on conversion of *n*-pentane over powdery and extruded CLD/Ga/Ac/ZP5 catalysts. (Reaction conditions: 500 °C, 1 atm, and WHSV= 5 $h^{-1}$)

Figure 4.17 shows that the extruded CLD/Ga/Ac/ZP5 catalyst had higher conversion and stability than its powdery form at the same zeolite content. It could be due to additional binder acidity and generated mesoporous matrices. At the same weight of catalyst, the Table 4.2 shows that the extruded CLD/Ga/Ac/ZP5 catalyst had lower Brønsted acidity (277 μmol/g) than its powder form (290 μmol/g) because

of lower zeolite content. In addition, BET surface area of extruded CLD/Ga/Ac/ZP5 (284 $m^2/g$) catalyst was also lower than its powder form (291 $m^2/g$) because extrudates containing gamma-$Al_2O_3$ have lower surface than HZSM-5 zeolite catalyst as shown in Table 4.1.

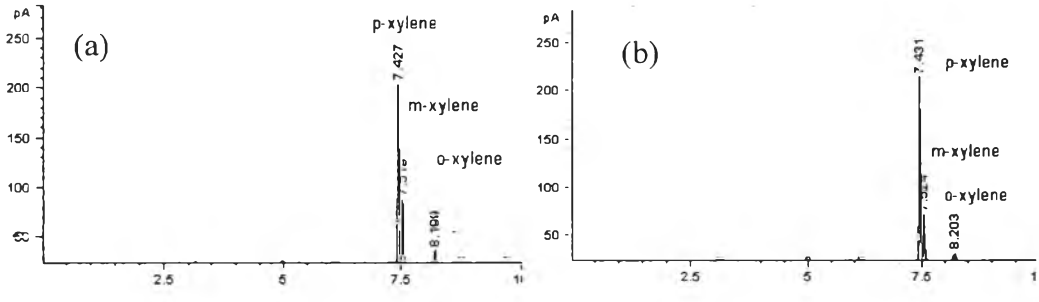


**Figure 4.18** Chromatogram of pulse *p*-xylene 5 µl at 500 °C and 1 atm over (a) Pseudoboehmite and (b) Silylated pseudoboehmite.

**Table 4.11** Product selectivity and conversion of *n*-pentane over unmodified HZSM-5, extruded CLD/Ga/Ac/ZP5 and CLD/Ga/Ac/ZP20 catalysts (Reaction condition: 500 °C, 1 atm, WHSV = 5 $h^{-1}$, and TOS = 440 min)

| Products | Catalysts | | |
|---|---|---|---|
| | HZSM-5 | Extruded CLD/Ga/Ac/ZP5 | Extruded CLD/Ga/Ac/ZP20 |
| Light paraffins | 16.07 | 5.79 | 3.21 |
| Light olefins | 9.43 | 7.78 | 4.78 |
| Benzene | 5.78 | 5.60 | 7.23 |
| Toluene | 28.48 | 34.90 | 36.71 |
| Ethylbenzene | 1.77 | 1.64 | 2.36 |
| Total Xylenes | 23.94 | 28.73 | 22.39 |
| *p*-Xylene | 5.61 | 14.42 | 11.87 |
| *m*-Xylene | 13.22 | 11.56 | 8.27 |
| *o*-Xylene | 5.10 | 2.75 | 2.25 |
| Others | 14.53 | 15.55 | 23.31 |
| Selectivity of Aromatics | 68.69 | 81.98 | 87.07 |
| Aromatics yield | 59.96 | 70.88 | 68.69 |
| Conversion | 87.29 | 86.46 | 78.89 |
| *p*-Xylene selectivity in xylenes | 23.44 | 50.20 | 53.02 |
| *p*-Xylene yield | 4.90 | 12.47 | 9.36 |

**Table 4.12** Mixed xylenes yield with pulse *p*-xylene 5 μl at 500 °C and 1 atm over pseudoboehmite binder

| Component | Yield (wt%) | |
|---|---|---|
| | Before silylation | After silylation |
| *p*-xylene | 75.7 | 79.3 |
| *m*-xylene | 21.1 | 18.1 |
| *o*-xylene | 3.2 | 2.6 |
| Total | 100.0 | 100.0 |

After silylation, the xylenes isomerization still occurred so that extruded catalysts performed lower *p*-xylene selectivity in xylenes than powdery catalysts. It could be acid sites from acetic acid and extraframework alumina species of $\gamma$-$Al_2O_3$ binder (Zhang *et al.* 2015).

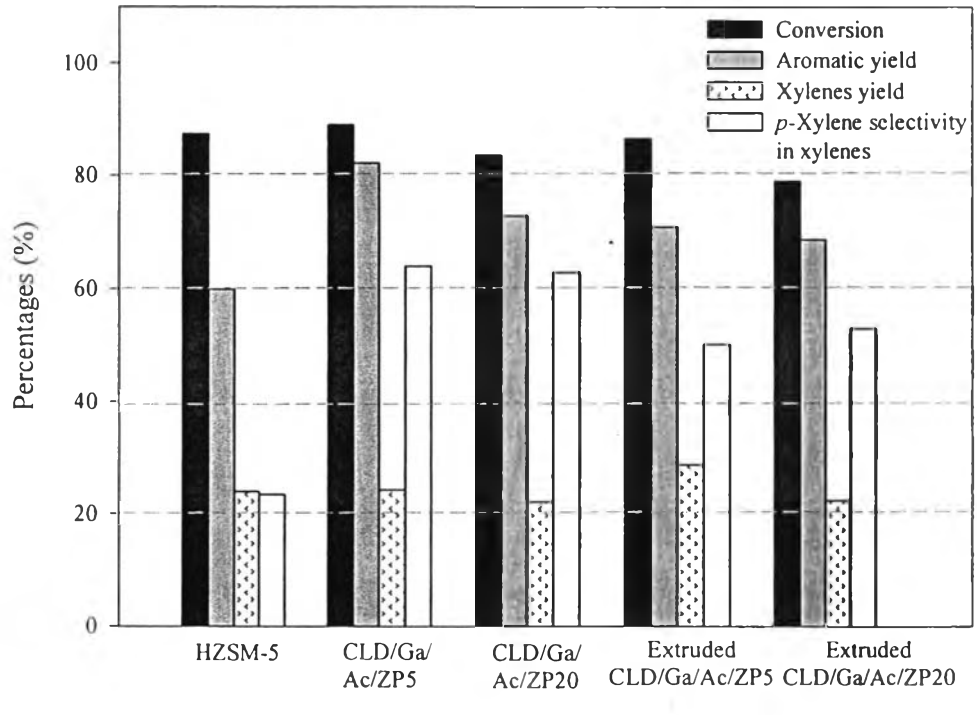


**Figure 4.19** Conversion of *n*-pentane, aromatic yield, xylenes yields, and p-xylene selectivity in xylenes of extruded HZSM-5 catalysts. (Reaction condition: 500 °C, 1 atm, WHSV = 5 $h^{-1}$, and TOS = 440 min)

Figure 4.20 shows that the spent CLD/Ga/Ac/ZP5 extrudates catalyst had lower coke formation (3.3 wt%) than the spent CLD/Ga/Ac/ZP5 catalyst (4.3 wt%) because of binder matrices. The spent modified and extruded HZSM-5 catalysts exhibited lower amount of coke than as-received HZSM-5 catalyst with 7.7 %coke. In agreement with Niwa and co-worker in 2012, the mild steaming treatment generated mesopore resulting low coke formation. According to Figure 4.20, most of coke formations were observed at high temperatures (500-800 °C) that would be the coke in internal pore. The coke formation on external pore and near the pore mouth region occurred at lower temperatures (200-400 °C). For extrudates, the peak was at 500 °C that could be the coke formation at the binder.

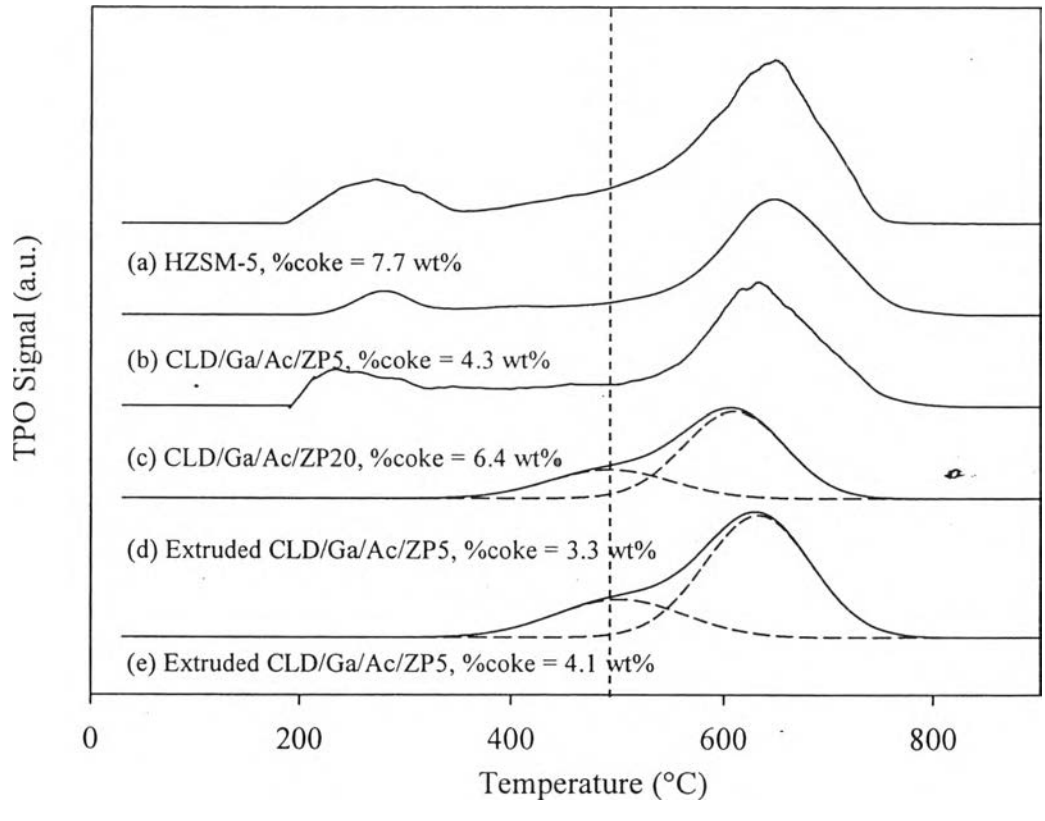


**Figure 4.20** Temperature programmed oxidation (TPO) profiles of spent CLD/Ga/Ac/ZP5 and CLD/Ga/Ac/ZP20 catalysts in powder and extrudates after 440 min time on stream. (Reaction condition: 500 °C, 1 atm, and WHSV = 5 $h^{-1}$)

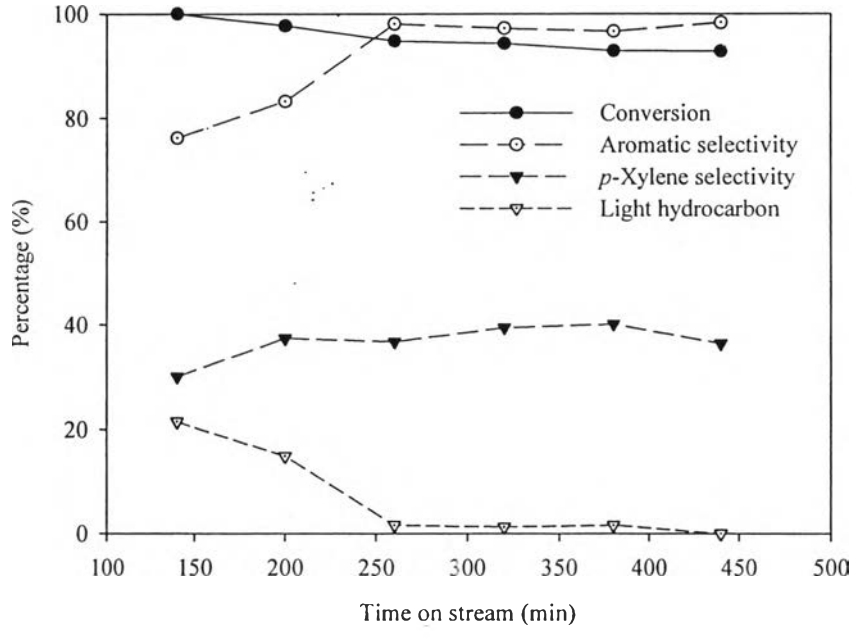


**Figure 4.21** Light naphtha conversion, aromatic selectivity, *p*-xylene selectivity in xylenes, and light hydrocarbons yield over extruded CLD/Ga/Ac/ZP5 catalyst. (Reaction conditions: 500 °C, 1 atm, and WHSV = 2 $h^{-1}$)

To apply for industrial condition, the extruded CLD/Ga/Ac/ZP5 catalyst was carried out at 500 °C, 1 atm, light naphtha feed, and WHSV = 2 $h^{-1}$. Table 4.13 shows the light naphtha 92.9 wt% conversion and 12.9 wt% *p*-xylene yield. According to Figure 4.21, aromatics selectivity was stable after 260 min time on stream because of the decreased formation of light hydrocarbon. It could be that fresh catalyst had excessive active sites preferring cracking reaction than aromatization.

**Table 4.13** Product yield of the extruded CLD/Ga/Ac/ZP5 catalyst (Reaction condition: 500 °C, 1 atm, WHSV = 2 $h^{-1}$, and TOS = 140 and 440 min)

| **Product yield (wt%)** | | **Time on stream (min)** | |
|---|---|---|---|
| **Component** | **Feed** | **140** | **440** |
| Light paraffins | - | 9.1 | 0.0 |
| Light olefins | - | 12.3 | 0.0 |
| Pentane | 75.0 | 0.0 | 7.1 |
| Hexane | 25.0 | 0.4 | 0.0 |
| Benzene | - | 28.8 | 33.0 |
| Toluene | - | 28.6 | 37.1 |
| Ethylbenzene | - | 0.0 | 0.0 |
| Total Xylenes | - | 18.8 | 21.2 |
| *p*-Xylene | - | 11.5 | 13.9 |
| *m*-Xylene | - | 5.2 | 5.5 |
| *o*-Xylene | - | 2.1 | 1.9 |
| Selectivity of aromatics | - | 76.2 | 98.3 |
| Selectivity of *p*-xylene in xylenes | - | 61.1 | 65.4 |
| Conversion | - | 100.0 | 92.9 |
| *p*-Xylene yield | - | 11.5 | 12.9 |